DOI: 10.1002/chem.201001417

Sexithiophene Encapsulated in a Single-Walled Carbon Nanotube: An In Situ Raman Spectroelectrochemical Study of a Peapod Structure

Martin Kalbáč,*[a, b] Ladislav Kavan,[a] Sandeep Gorantla,[c] Thomas Gemming,[c] and Lothar Dunsch[b]

Abstract: The interaction of single-walled carbon nanotubes (SWCNTs) and α-sexithiophene (6T) was studied by Raman spectroscopy and by in situ Raman spectroelectrochemistry. The encapsulation of 6T in SWCNT and its interaction causes a bleaching of its photoluminescence, and also small shifts of its Raman bands. The Raman features of the SWCNT with embedded 6T (6T-peapods) change in both intensity and frequency compared to those of pristine SWCNT, which is a consequence of a change of the resonant condition. Electrochemical doping demonstrated that the electrode potential applied to the SWCNT wall causes changes in the embedded 6T. The effects of electrochemical charging on the Raman features of pristine SWCNT and 6T@SWCNT were compared. It is shown that the interaction of SWCNT with 6T also changes the electronic structure of SWCNT in its charged state. This change of electronic structure is demonstrated both for semiconducting and metallic tubes.

Keywords: doping · electrochemistry · nanotubes · Raman spectroscopy · sexithiophene

Introduction

Oligothiophenes as organic semiconductors[1,2] are good candidates for applications in electronics and devices such as organic field effect transistors[3] or solar cells.[4] Among oligothiophenes, α-sexithiophene (6T) is particularly attractive due to its high hole mobility in the solid state.[5]

It has been shown recently that the morphology of 6T influences the performance of devices dramatically.[6] However, it is very difficult to control the morphology in macroscopic crystals. The assembly of crystals inside single-walled carbon nanotubes (SWCNTs) presents a challenge for this control, because unusual crystal structures of many inorganic materials can be grown in this way.[7] The diameter of SWCNTs is typically in the range of 1–2 nm. This is comparable to the size of small organic molecules, which can therefore be confined in the interior of SWCNTs. However, for applications in electronics it is also very important to understand the electronic exchange between 6T and SWCNT in the peapod structures, 6T@SWCNT.

In situ spectroelectrochemistry is the method of choice for studying carbon nanostructures,[8–13] because characterization of the electronic structure of these materials both in the neutral and charged states is possible upon electrochemical doping. We have shown recently that the electronic structure of SWCNT is very sensitive to doping, resulting in significant changes in their Raman spectra.[14] These changes are reversible and reproducible for a selected SWCNT sample.[15,16] Hence, SWCNTs can also be used as in situ probes for studies of hybrid materials like SWCNT/polymer composites[17,18] and/or to monitor the electronic structure of species encapsulated inside SWCNTs.[19,20] The SWCNTs are stable in a relatively wide potential window. Thus, the interaction of many hybrid materials based on SWCNT in a charged state can be evaluated by this probe.

[a] Dr. M. Kalbáč, Prof. L. Kavan
J. Heyrovský Institute of Physical Chemistry
v.v.i., Academy of Sciences of the Czech Republic
Dolejškova 3, 18223 Prague 8 (Czech Republic)
Fax: (+420) 2-8658-2307
E-mail: kalbac@jh-inst.cas.cz

[b] Dr. M. Kalbáč, Prof. Dr. L. Dunsch
Center of Spectroelectrochemsitry
Department of Electrochemistry and Conducting Polymers
Leibniz-Institute of Solid State and
Materials Research (IFW Dresden)
Helmholtzstr. 20, 01069 Dresden (Germany)

[c] S. Gorantla, Dr. T. Gemming
Institute of Complex Materials
Leibniz-Institute of Solid State and
Materials Research (IFW Dresden)
Helmholtzstr. 20, 01069 Dresden (Germany)

Supporting information for this article is available on the WWW under http://dx.doi.org/10.1002/chem.201001417.

 © 2010 Wiley-VCH Verlag GmbH & Co. KGaA, Weinheim View this journal online at wileyonlinelibrary.com

For SWCNTs it is convenient to combine electrochemistry with Raman spectroscopy, as the latter is frequently used as a tool for the characterization of nanotube samples. In addition, it provides a sensitive reflection of the changes in nanotubes induced by doping. The main features of the Raman spectra of SWCNTs include the radial breathing mode (RBM), the tangential mode (TG), the D mode and the G′ mode (also known as the 2D or the D* mode). The D band in the Raman spectra is a signature of defects. The RBM frequency is proportional to the inverse diameter of the SWCNT.

Due to the one-dimensional nature of SWCNTs, their density of states (DOS) exhibits characteristic Van Hove singularities, the positions of which depend only on the SWCNT diameter and chirality. The singularities provide strong resonant enhancement of the otherwise weak Raman signal. The resonance window, which determines which specific chiralities will appear in a RBM spectrum excited at a given excitation wavelength, varies from tens of meV for a single nanotube to >140 meV for bundles of nanotubes. RBMs from nanotubes outside the resonance window of a selected excitation wavelength will not be observed, so only a very small set of tubes of the samples participates in the Raman scattering for a single excitation line.

Raman spectroscopy has also been used for studies of oligothiophenes, including 6T in its neutral or charged state.[21,22] Apart from structural information[23,24] it is possible to distinguish the cation and dication structures of the oligothiophene from the neutral molecules.[21,22]

In this work, we applied in situ Raman spectroelectrochemistry to control and characterize the doping level of 6T@SWCNT. The 6T embedded in SWCNT exhibited an improved stability with respect to that of pristine 6T, which allowed us to perform studies in a relatively large potential range (from -1.2 to 1.5 V vs. Ag/Ag^+ pseudo-reference). We show here for the first time that the electrochemical doping of 6T@SWCNT causes a reversible bleaching of the Raman signals of both 6T and SWCNT, thus both structures can be tuned by electrochemical charging. Nevertheless, the interaction of 6T and SWCNT also leads to changes in their electronic structures, which in turn influence the course of the electrochemical doping of 6T@SWCNT. This finding is important for future applications of the 6T@SWCNT heterostructure in devices.

Results and Discussion

High-resolution transmission electron microscopy (HRTEM) images of 6T@SWCNT are shown in Figure 1. HRTEM imaging was performed with a relatively low electron energy of 80 keV to limit specimen damage by radiation. The necessary high resolution was maintained by hardware correction of the spherical aberration of the objective lens. With this, we were able to obtain images of 6T molecules inside SWCNT up to atomic resolution. Figure 1 shows a time series of 6T molecules in SWCNT of diameter

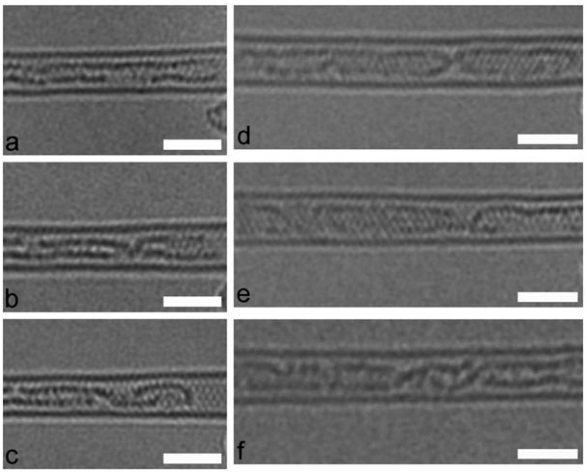

Figure 1. The left and right panels show time series of HRTEM images of 6T@SWCNT with diameters of 1.32 nm and 1.5 nm, respectively. The time difference between the images is 1 s, except between b) and c) where it is 7 s. The length of the scale bar is 2 nm.

1.32 nm (left) and 1.5 nm (right). The time difference between the images is 1 s, but between b) and c) it is 7 s. The images show that the 6T@SWCNT can rotate during prolonged electron bombardment. The mean distance between the molecule and the tube wall is in the range of 0.38–0.39 nm in both cases, independent of the tube diameter. This agrees well with the lowest energy spacing of about 0.4 nm calculated theoretically in reference [25]. We note that in the latter work the experimental spacing was found to be between 0.32 and 0.35 nm.

In general, the estimation of the filling factor of the peapod is difficult. Nevertheless, based on the HRTEM and Raman spectroscopy measurements (see below in this section) we estimate more than half of the tubes to be filled. The expected effect of the filling factor on spectroscopy is only a change in the intensities of the Raman features, brought about simply by reducing the amount of material which contributes to the Raman spectra. Other changes are not expected.

It is also difficult to exclude some 6T molecules remaining adsorbed on the outer wall of SWCNT. On the other hand, the stability of the Raman features of 6T during the electrochemical treatment of the sample suggests that contributions of non-encapsulated 6T to the Raman signal are small (a more detailed discussion is given below).

Figure 2 shows a comparison of the Raman spectra of 6T, SWCNT and 6T@SWCNT. The spectra are excited by 1.83 eV laser energy. Note that for pure 6T we observed a strong photoluminescence and the stability of the material was limited, which did not allow the collection of spectra under the same conditions as for SWCNT and 6T@SWCNT. Hence, the Raman spectra of 6T were excited by a laser power ten times lower. The photoluminescence background is present even at reduced laser power, but it was removed for convenience. Note that for 6T the photoluminescence background was observed also at other laser excitation ener-

 © 2010 Wiley-VCH Verlag GmbH & Co. KGaA, Weinheim

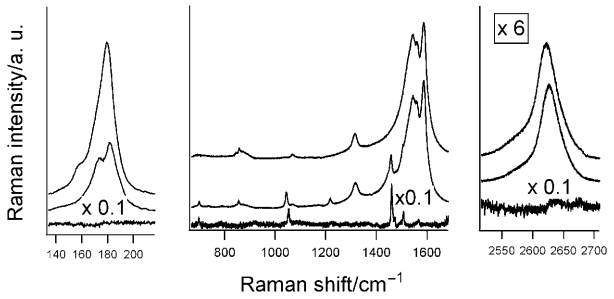

Figure 2. The Raman spectra of 6T, 6T@SWCNT and SWCNT (from bottom to top). The spectra were excited using the 1.83 eV laser excitation energy. Note that for the spectrum of 6T the photoluminescence background was removed. Furthermore, for 6T the laser power was 10 times lower to prevent burning of the material and to avoid detector saturation due to strong photoluminescence of 6T.

gies (data not shown). However, in the case of 6T@SWCNT peapod the photoluminescence background was absent.

The Raman spectra of SWCNT in Figure 2 exhibit the RBM band position between 175 and 190 cm^{-1}, which gives the diameter of our tubes as ≈1.3–1.5 nm. According to the Kataura plot,[26] optical transitions in 1.3–1.5 nm metallic tubes resonate with the 1.83 eV laser excitation energy. Indeed, the TG mode exhibits a Breit–Wigner–Fano (BWF) broadening typical for metallic tubes.

The Raman spectra of 6T are more complicated. The main Raman features were found between 650 and 1600 cm^{-1}. The bands were tentatively assigned according to previous studies:[23,24] the band at 697 cm^{-1} to C-S-C deformation, the band at 1051 cm^{-1} to C–H bending, the band at 1220 cm^{-1} to C–C inter-ring stretching, and two bands at 1461 cm^{-1} and 1504 cm^{-1} to C=C intra-ring stretching vibrations.

The Raman spectra of the 6T@SWCNT correspond to a rough superposition of the spectra of SWCNTs and 6T, respectively. However, a more detailed analysis points to several differences which are specific for the interactions between the 6T and SWCNTs in peapods.

As already mentioned, a remarkable effect is the absence of the photoluminescence background in the spectra of 6T@SWCNT compared to pristine 6T. The absence of photoluminescence can be rationalized assuming that exciton energy transfer from 6T to SWCNT takes place. The sample contains both semiconducting and metallic tubes. The presence of metallic tubes in the sample causes a quenching of the photoluminescence. Hence, the exciton energy transferred to the nanotubes is suggested to be preferentially dissipated by non-radiative channels. We note that for pristine molecules the photoluminescence is very strong, hence even small amounts of non-interacting 6T would result in a significant background in the Raman spectra, which is not observed experimentally, so it follows that most of the 6T molecules are inside the SWCNT.

The Raman bands of 6T reflect the interaction with SWCNT. Their intensity is dramatically reduced (note that the Raman spectra of pristine 6T were excited by laser power reduced by a factor of ten). The change in intensity is often observed for encapsulated species because the intratubular molecule is screened by the nanotube wall. Also, the frequencies of the Raman bands are changed. However, these changes are different, even in their trends. Some bands are downshifted, for example, the 6T bands at 1054 and 1462 cm^{-1} downshift to 1045 and 1459 cm^{-1}, respectively, in 6T@SWCNT. On the other hand, an upshift in the Raman frequency is observed, for example, the Raman band at 698 cm^{-1} upshifts to 700 cm^{-1}. Similar changes may occur for the other Raman bands of 6T too, but their intensities are weak, so it is difficult to follow changes in their frequency.

The Raman features of carbon nanotubes decrease in their intensities for the 6T@SWCNT compared to pristine SWCNT, which is probably due to the absorption of the incident and scattered light (the Raman signal from SWCNTs) by encapsulated 6T. Furthermore, there are significant changes in the line shape and frequencies of the nanotube Raman bands.

Whereas for the pristine sample the spectra are dominated by the RBM band centered at about 180 cm^{-1}, for 6T@SWCNT we found two bands centered at 173 and 182 cm^{-1}. It has been shown previously that the filling of SWCNT has a significant impact on the RBM band.[27] In a previous study of C_{60}@SWCNT the observed changes in the RBM band were explained by mechanical hindrance, and also by the interaction of near-free electron states of SWCNT with encapsulated molecules.[27] The mechanical interaction is not expected for 6T because its size is too small compared to the nanotube diameter. Hence, the modification of the electronic structure of SWCNT by interaction with 6T seems to be a reason for the change in the RBM band frequency.

The shape of the TG mode of metallic SWCNT is very sensitive to doping, as shown previously.[28,29] However, here we found only a very slight difference between the TG mode of SWCNT and 6T@SWCNT. Therefore, the charge transfer between SWCNT and encapsulated 6T is not significant. This is in contrast to SWCNT/polymer composites, for which a relatively large charge transfer has been found.[18] The reason could be that the 6T is encapsulated inside the SWCNT. The inner space of the nanotube is probably more intact, and complete charge transfer is thus limited.

The G′ mode of the 6T@SWCNT is upshifted by about 5 cm^{-1} with respect to the frequency in empty SWCNT, which may also be a consequence of a change in resonance condition.

Spectroelectrochemical experiments: To follow the possibilities of tuning the electronic structure of 6T encapsulated inside SWCNT, and to study the changes in the electronic structure of SWCNTs in detail, we performed a series of in situ Raman spectroelectrochemical measurements.

Figure 3 shows the Raman spectra of pristine 6T@SWCNT using a 1.83 eV laser excitation energy. The development of the Raman spectra of pristine SWCNT at the

 © 2010 Wiley-VCH Verlag GmbH & Co. KGaA, Weinheim

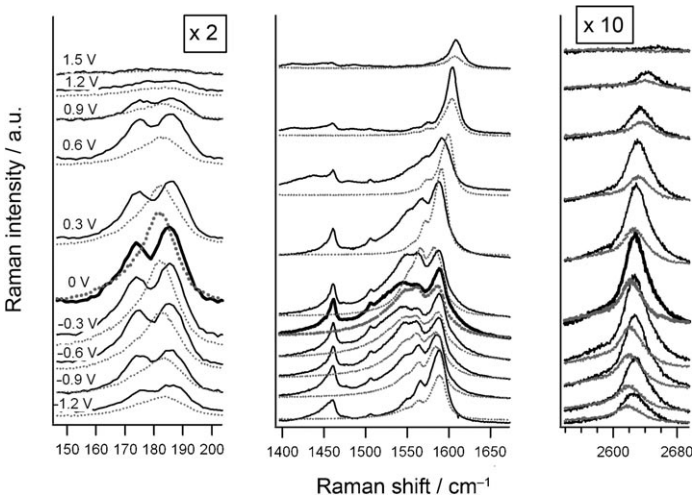

Figure 3. Potential-dependent Raman spectra (excited at 1.83 eV) of 6T@SWCNT (solid line) and pure SWCNT (dotted line) on a Pt electrode in 0.2 M $LiClO_4$ + acetonitrile. The electrode potential was varied by steps of 0.3 V from 1.5 to −1.2 V vs. Ag pseudo-reference electrode for curves from top to bottom. Spectra are offset for clarity, but the intensity scale is identical for all spectra in the respective window.

same potentials and the same laser excitation energy is also shown for comparison. (The spectroelectrochemical measurement of pristine 6T was complicated by a strong photoluminescence background and limited stability of the 6T film on the electrode. Hence, we do not show and analyze these data here.)

The measurements were always started at an electrode potential of 0 V, which was close to the open circuit potential, to minimize the change of the electronic structure and the doping level of the components at the beginning of the electrochemical study. The potential was changed in the sequence: +0.3, −0.3, +0.6, −0.6, +0.9, −0.9, +1.2, −1.2 and +1.5 V. At each step, the Raman spectra were recorded while keeping the potential constant. Almost no current flow was observed during the collection of the Raman spectra, which shows that the spectra were recorded at the quasi-equilibrium state.

The main effect of the electrochemical doping of SWCNTs is a subsequent bleaching of the nanotube Raman modes (RBM, TG and G′ modes). The bleaching of SWCNT modes during charging is in agreement with previously published results.[10,28] The electrochemical doping leads to a shift of the Fermi level. Thus, the Van Hove singularities are filled/depleted upon cathodic/anodic charging. The simple model assumes that the filling/depletion of the Van Hove singularities which are involved in the resonant Raman process induce the loss of the resonance Raman enhancement due to the loss of optical absorptions between these particular Van Hove singularities. The loss of resonant enhancement leads to the observed bleaching of all SWCNT features. However, this mechanism has recently been revised, as a significant bleaching of Raman bands is observed before the Fermi level reaches the Van Hove singularity, which is in resonance with excitation laser energy. This effect is observed both in bundles[15,30] and for single nanotubes.[14] Hence, it was suggested that the filling of any electronic state of SWCNT changes its whole electronic structure due to the charge-induced broadening of Van Hove singularities.[14,15] This is particularly important for metallic tubes. Because the metallic tubes do not have a band gap (or the band gap is very small), even a weak doping can influence the electronic properties significantly.

In addition, for metallic tubes the TG mode is affected by the Kohn anomaly,[31] which is also sensitive to doping. The effect of a plasmon should also be considered for nanotube bundles.[16] These effects cause a complex but reproducible change of the line-shape of the TG band for even a small change in the doping level.[16,32] The high sensitivity of the TG mode to the charging designates this mode as a probe for the studies of the interactions between SWCNT and other materials. The comparison of the TG mode shape in the Raman spectra of 6T@SWCNT with reference to spectra of SWCNT may thus disclose the influence of the encapsulated 6T on the doping behavior of the nanotube, as discussed below in this section.

A comparison of the Raman features of the 6T@SWCNT and those of the empty SWCNT does not reveal dramatic differences, which confirms that the effect of encapsulated 6T on SWCNT is relatively weak. However, a careful analysis of the Raman spectra at different electrode potentials shows several differences in the behavior of empty and 6T-filled SWCNT. The RBM mode in 6T@SWCNT is less sensitive to electrochemical doping. At an electrode potential of 0 V the intensity of the RBM band in empty SWCNT is significantly stronger than that of 6T@SWCNT. However, at potentials of about 0.3 and −0.6 V, the RBM bands have comparable intensities for both samples. At even higher magnitudes of electrode potentials the intensity of the RBM band is clearly weaker than that of 6T@SWCNT. The RBM mode in 6T@SWCNT keeps the double-peak structure. At very high potentials (+1.5 or −1.2 V) it is difficult to distinguish two bands, but this is more likely to be due to the very low intensity of these bands, and not to the merging of the bands into one. Therefore, the splitting of the RBM band in 6T@SWCNT cannot simply be explained by a charge transfer. This is because a pure charge transfer interaction of 6T with SWCNT would be compensated at increased electrode potential. In other words, at a certain electrode potential the spectra of the SWCNT part of 6T@SWCNT would be the same as the spectra of pristine SWCNT. However, this is not the case. Hence, a more complex interaction (such as the hybridization of 6T electronic orbitals with the nanotube's near-free electron states) must be considered.[27]

The development of the TG mode is also different for empty SWCNT and 6T@SWCNT. A very sensitive lower-frequency part of the TG mode disappears much faster for a pristine SWCNT sample than for 6T@SWCNT. This is in agreement with the RBM band behavior. A comparison of the spectral line shape suggests that the "delay" in the line-shape change is about 0.3 V. (For example, the spectrum of

 © 2010 Wiley-VCH Verlag GmbH & Co. KGaA, Weinheim

6T@SWCNT at +0.9 V is similar to the spectrum of the pristine SWCNT at 0.6 V.)

The G′ band intensity of empty SWCNT is bleached slightly faster than in the case of a 6T@SWCNT sample, which is consistent with the behavior of other Raman features. In addition, there is a difference in the shift of the G′ band for SWCNT and 6T@SWCNT. It is clear for both the positive doping and the negative doping that changes of the frequency are significantly slower for 6T@SWCNT than for SWCNT. This is consistent with the behavior of other Raman bands. The frequency of the G′ band at 0 V is 2627 and 2622 cm^{-1} for 6T@SWCNT and SWCNT, respectively. However, at a potential of 1.2 V, the frequency of the G′ mode for empty SWCNT is about 2641 cm^{-1} and for 6T@SWCNT about 2643 cm^{-1}. At a potential of −1.2 V, the frequency of the G′ mode for empty SWCNT is about 2619 cm^{-1}, and for 6T@SWCNT about 2626 cm^{-1}.

The Raman bands of 6T in 6T@SWCNT lose their intensity upon electrochemical charging. This demonstrates that the molecules inside SWCNT are indeed affected by the electrode potential. However, the intensity of the Raman signal can be recovered if the electrode potential is returned to that of the uncharged state at 0 V. This is a clear manifestation of the exceptional stability of the encapsulated 6T. The nanotube wall is capable of transferring the charge, but it protects the 6T molecule from the environment. It is also intact enough to ensure that the irreversible functionalization of the inner wall of SWCNT by chemical reaction with 6T does not occur. An improved stability of species encapsulated in SWCNT was observed previously on a beta-carotene sample.[33] We assume that if some residual 6T was located outside the SWCNTs, it would be decomposed by our electrochemical treatment. Hence, the contribution from these molecules to the Raman spectra of the sample after electrochemical treatment would be negligible or absent.

In contrast to a remarkable intensity change, the frequency of the 6T Raman bands is not changed. The pristine 6T may form a cation or dication upon p-doping, which was also demonstrated previously by Raman spectroscopy.[22] The formation of the cation, and also the dication, is associated with a change in both the frequency and intensity of the Raman features compared to the neutral molecule. As in our case of 6T@SWCNT we did not observe a significant change of the Raman frequency, complete charge transfer and the formation of cation/dication can be ruled out. On the other hand, we observed a change of the Raman intensity in doped 6T@SWCNT. This can be related to the change in the resonance, which is more sensitive to doping. Our results are consistent with previous studies on fullerene peapods.[19,20,34] In these cases, no direct charge transfer from the fullerene to the SWCNT was observed during electrochemical charging. The C_{70} features in C_{70}@SWCNT peapods mimic the behavior of 6T@SWCNT.[34] There is also a significant attenuation of the Raman intensity, but the change in frequency does not indicate any formation of C_{70}^{+} or C_{70}^{-}.[34] In the case of C_{60}, the pentagonal pinch $A_g(2)$ mode frequency of C_{60} is very sensitive to doping, and can even be used to calculate the number of electrons transferred on the C_{60} cage.[35] Nevertheless, in the case of the electrochemical doping of C_{60}@SWCNT, only a very weak change of the $A_g(2)$ mode frequency was observed, which corresponds to a charge of a fraction of the electron.[34] For cathodic doping the intensity of the $A_g(2)$ mode is attenuated as expected, but for anodic doping the intensity of the $A_g(2)$ mode is anomalously increased. This behavior results from a complex interaction between the encapsulated species and the SWCNTs.[34]

We note that the bleaching of 6T Raman bands in 6T@SWCNT is much stronger for anodic doping. This is consistent with the redox behavior of pristine 6T, because the oxidation is relatively easy compared to reduction. Hence, this situation is opposite to that for fullerenes. From this point of view, the comparison of fullerene and oligothiophene peapods is particularly interesting.

Figure 4 shows in situ Raman spectroelectrochemical measurements of 6T@SWCNT excited by 2.54 eV laser energy. According to the Kataura plot, the semiconducting

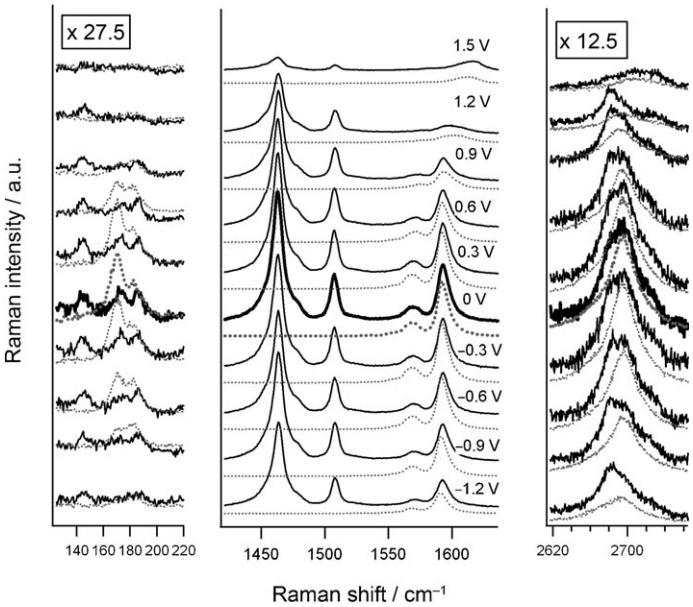

Figure 4. Potential-dependent Raman spectra (excited at 2.54 eV) of 6T@SWCNT (solid line) and pristine SWCNT (dotted line) on a Pt electrode in 0.2 M $LiClO_4$ + acetonitrile. The electrode potential was varied by steps of 0.3 V from 1.5 to −1.2 V vs. Ag pseudo-reference electrode for curves from top to bottom. Spectra are offset for clarity, but the intensity scale is identical for all spectra in the respective window.

tubes are in resonance with the 2.54 eV laser energy in our sample. The RBM band region is significantly different for 6T@SWCNT and SWCNT. This is consistent with the data shown in Figure 3, in which these changes were assigned to the different resonance conditions of the nanotubes in the 6T@SWCNT sample. The RBM bands of pristine SWCNT are bleached faster than for 6T@SWCNT. At an electrode potential of 0 V the Raman signals of the RBM bands between 180–200 cm^{-1} are at least twice as strong for pristine

 © 2010 Wiley-VCH Verlag GmbH & Co. KGaA, Weinheim

SWCNT than for 6T@SWCNT. However, at potentials of ± 0.9 V, both samples exhibit a similar intensity of the RBM bands from 180–200 cm^{-1}. This behavior indicates that the semiconducting tubes are affected by encapsulation of 6T in the same way as metallic tubes.

The bleaching behavior of the TG mode of the 6T-filled semiconducting SWCNT is quite similar to that of the pristine semiconducting SWCNT tube. In the case of semiconducting nanotubes the Kohn anomaly is absent, so changes in the electronic structure are reflected only by the change in the intensity of the Raman bands at low electrode potentials. Nevertheless, if the electrode potential exceeds ± 0.9 V, a change in frequency of the TG mode is also observed. As demonstrated recently, the frequency change results from a competition of the phonon renormalization effect and the C–C spring force.[36] The change of spring constant is dependent on the nanotube diameter. Therefore, the magnitude and even the sign of the frequency shifts are dependent on the nanotube diameter. Bundles of SWCNTs usually contain many different tubes, but due to the resonance enhancement only a fraction of these tubes contributes to the Raman spectra excited by a certain laser energy. In other words, different laser excitation energies will excite tubes with different diameters exhibiting a different dependence on electrode potential. Because different tubes are in resonance for 6T@SWCNT and pristine SWCNT, a different dependence of the TG mode on the electrode potential can also be expected. Nevertheless, the general trend is a downshift at negative potentials and an upshift at positive electrode potentials observed for both the SWCNT and 6T@SWCNT.

The G′ mode is less attenuated for 6T@SWCNT than for pristine SWCNT. This is consistent with other Raman features and also with the data obtained at 1.83 eV laser energy. The G′ mode of 6T exhibits a double-peak structure and a dependence on nanotube diameter. As tubes in a broader diameter range are in resonance (this is also clear from the RBM mode, where more bands appear as compared to unfilled tubes), a broader or more complex G′ mode can also be expected. The change of the G′ mode can be alternatively explained by a shift of the resonance maxima of filled SWCNTs.

For 2.54 eV laser excitation energy 6T is itself close to its resonance condition, and therefore the Raman signal of 6T dominates these spectra. Nevertheless, the dependence of the Raman intensity on electrode potential is similar to that for 1.83 eV laser energy. The asymmetry of the bleaching behavior with respect to the sign of the electrode potential is also reproduced. Hence, the resonance does not play a significant role in the behavior of embedded 6T during electrochemical charging.

The doping experiments have clearly shown that the properties of the 6T@SWCNT are not due to a simple superposition of the properties of its components, that is, 6T and SWCNT. This can be crucial in applications for which precise control of the doping level is necessary. The most evident effect is a delayed bleaching of the SWCNT bands in the 6T@SWCNT.

The 6T inside SWCNT can influence the electronic structure of the SWCNTs. It has been shown that electrochemical doping results in a broadening of Van Hove singularities.[14] This effect can be also responsible for a different behavior of SWCNT and 6T@SWCNT in electrochemical charging. If the singularities are broadened due to electronic interaction between 6T and SWCNT, the effect of the charge on the bleaching of the Raman signal is weakened, and is visible over a wider range of electrode potentials.

Conclusion

We prepared 6T@SWCNT peapods from 6T and SWCNT by thermal reaction. The resulting material was studied by Raman spectroscopy and in situ Raman spectroelectrochemistry. The interaction of encapsulated 6T and SWCNT caused changes in the Raman spectra of both 6T and SWCNT. After encapsulation of 6T inside SWCNT, the Raman spectra exhibited different bands in the RBM region. This suggests a different resonance condition of filled SWCNT compared to pristine SWCNT. The diameter distribution of filled SWCNTs in resonance has also been suggested to be different from that of empty SWCNTs by analysis of the G′ band. The 6T Raman features were slightly shifted with respect to the positions in pristine 6T. The strong photoluminescence of 6T was also quenched by interaction with SWCNT.

In addition, the in situ Raman spectroelectrochemical data of 6T@SWCNT excited by two different laser excitation energies (2.54 and 1.83 eV) have been discussed in detail; these probed the semiconducting and metallic tubes in our sample, respectively. We found that 6T can be doped and changed even if it is embedded inside SWCNT. Nevertheless, the doping effect is observed for 6T only at relatively high electrode potentials. On the other hand, the formation of the 6T cation/dication has not been observed during electrochemical doping. The interaction of 6T and SWCNT leads to the different dependence of the Raman intensity of the nanotube bands on electrode potential. The most significant effect was a slower bleaching of the Raman bands of 6T@SWCNT compared to pristine SWCNT during electrochemical doping. The delayed attenuation of the Raman features of 6T@SWCNT is in agreement with previous studies on SWCNT/polymer composites, and may be explained by a change of the electronic structure of SWCNT, including a broadening of Van Hove singularities.

Experimental Section

Peapods 6T@SWCNT were prepared by heating of 6T (Aldrich) and SWCNT (laser ablation) in a glass ampoule in vacuum (10^{-6} mbar) at about 200 °C for 8 h. The resulting peapod samples were washed with an excess of CH_2Cl_2, in which 6T is soluble. At the beginning of the washing procedure we detected that some 6T was removed. If the filtrate was colorless we sonicated the sample in an excess of solvent. Hence, only very little (if any) 6T could be located outside the SWCNT, and the contribu-

 © 2010 Wiley-VCH Verlag GmbH & Co. KGaA, Weinheim

tion from these molecules to the Raman spectra of the sample would be negligible.

Thin-film SWCNT and 6T@SWCNT electrodes were prepared by evaporation of the sonicated (approximately 15 min.) ethanolic slurry of the SWCNT or 6T@SWCNT on a Pt electrode in air. The film electrodes were out-gassed overnight at 90 °C in vacuum and then mounted in a spectroelectrochemical cell in a glove box. The cell was equipped with a Pt counter electrode and an Ag wire pseudo-reference electrode. 0.2 M $LiClO_4$ in dry acetonitrile was used as the supporting electrolyte solution. Electrochemical experiments were controlled by a PG 300 (HEKA) or EG&G PAR 273 A potentiostat.

HRTEM was carried out with a Titan 80-300 (FEI), using a corrector for the spherical aberration of the objective lens. For imaging, an electron energy of 80 keV was used to minimize specimen damage. Despite the relatively low electron energy the corrector enables a high resolution sufficient to image the projected C–C distance of the SWCNT.

The Raman spectra were measured on a T-64000 spectrometer (Instruments SA) interfaced to an Olympus BH2 microscope, and by a Labram HR spectrometer (Horiba Jobin Yvon) interfaced to an Olympus BX-41 microscope (the laser power impinging on the sample or cell window was between 0.1–5 mW). Spectra were excited by a Kr^+ and an Ar^+ laser at 1.83 eV and 2.54 eV, respectively (Innova 305, Coherent). The Raman spectrometer was calibrated before each set of measurements by using the F_{1g} line of Si at 520.2 cm^{-1}. The spot size was $\approx 0.1 \times 0.1$ mm^2.

Acknowledgements

This work was supported by the GACR-DFG project (contract No. 203/07/J067). We thank Frank Ziegs and Christine Malbrich for technical help, and Evgenija Dmitrieva (all of IFW Dresden) for helpful discussions.

[1] A. J. Heeger, S. Kivelson, J. R. Schrieffer, W. P. Su, *Rev. Mod. Phys.* **1988**, *60*, 781–850.
[2] D. Fichou, *J. Mater. Chem.* **2000**, *10*, 571–588.
[3] M. Mushrush, A. Facchetti, M. Lefenfeld, H. E. Katz, T. J. Marks, *J. Am. Chem. Soc.* **2003**, *125*, 9414–9423.
[4] K. Hara, Z. S. Wang, T. Sato, A. Furube, R. Katoh, H. Sugihara, Y. Dan-Oh, C. Kasada, A. Shinpo, S. Suga, *J. Phys. Chem. B* **2005**, *109*, 15476–15482.
[5] F. Dinelli, M. Murgia, F. Biscarini, D. M. de Leeuw, *Synth. Met.* **2004**, *146*, 373–376.
[6] M. A. Loi, E. Da Como, F. Dinelli, M. Murgia, R. Zamboni, F. Biscarini, M. Muccini, *Nat. Mater.* **2005**, *4*, 81–85.
[7] M. Monthioux, *Carbon* **2002**, *40*, 1809–1823.
[8] M. Kalbac, L. Kavan, M. Zukalova, L. Dunsch, *Carbon* **2004**, *42*, 2915–2920.
[9] M. Kalbac, L. Kavan, M. Zukalova, L. Dunsch, *Adv. Funct. Mater.* **2005**, *15*, 418–426.
[10] L. Kavan, M. Kalbac, M. Zukalova, L. Dunsch, *J. Phys. Chem. B* **2005**, *109*, 19613–19619.
[11] P. Corio, A. Jorio, N. Demir, M. S. Dresselhaus, *Chem. Phys. Lett.* **2004**, *392*, 396–402.
[12] P. M. Rafailov, C. Thomsen, *J. Optoelectron. Adv. Mater.* **2005**, *7*, 461–464.
[13] M. Kalbac, A. A. Green, M. C. Hersam, L. Kavan, *ACS Nano* **2010**, *4*, 459–469.
[14] M. Kalbac, H. Farhat, L. Kavan, J. Kong, K. Sasaki, R. Saito, M. S. Dresselhaus, *ACS Nano* **2009**, *3*, 2320–2328.
[15] M. Kalbac, L. Kavan, L. Dunsch, *J. Phys. Chem. C* **2008**, *112*, 16759–16763.
[16] M. Kalbac, L. Kavan, L. Dunsch, M. S. Dresselhaus, *Nano Lett.* **2008**, *8*, 1257–1264.
[17] M. Kalbac, L. Kavan, L. Dunsch, *Compos. Sci. Technol.* **2009**, *69*, 1553–1557.
[18] M. Kalbac, L. Kavan, M. Zukalova, L. Dunsch, *Carbon* **2007**, *45*, 1463–1470.
[19] M. Kalbac, L. Kavan, M. Zukalova, L. Dunsch, *J. Phys. Chem. B* **2004**, *108*, 6275–6280.
[20] M. Kalbac, L. Kavan, M. Zukalova, L. Dunsch, *J. Phys. Chem. C* **2007**, *111*, 1079–1085.
[21] Y. Furukawa, N. Yokonuma, M. Tasumi, M. Kuroda, J. Nakayama, *Mol. Cryst. Liq. Cryst. Sci. Technol. Sect. A* **1994**, *256*, 113–120.
[22] N. Yokonuma, Y. Furukawa, M. Tasumi, M. Kuroda, J. Nakayama, *Chem. Phys. Lett.* **1996**, *255*, 431–436.
[23] J. R. Weinberg-Wolf, L. E. Mcneil, *Phys. Rev. B* **2004**, *69*, 1252021–4.
[24] A. Degli Esposti, M. Fanti, M. Muccini, C. Taliani, G. Ruani, *J. Chem. Phys.* **2000**, *112*, 5957–5969.
[25] M. A. Loi, J. Gao, F. Cordella, P. Blondeau, E. Menna, B. Bartova, C. Hebert, S. Lazar, G. A. Botton, M. Milko, C. Ambrosch-Draxl, *Adv. Mater.* **2010**, *22*, 1635–1639.
[26] H. Kataura, Y. Kumazawa, Y. Maniwa, I. Umezu, S. Suzuki, Y. Ohtsuka, Y. Achiba, *Synth. Met.* **1999**, *103*, 2555–2558.
[27] S. K. Joung, T. Okazaki, N. Kishi, S. Okada, S. Bandow, S. Iijima, *Phys. Rev. Lett.* **2009**, *103*, 027403–1–027403–4.
[28] L. Kavan, P. Rapta, L. Dunsch, *Chem. Phys. Lett.* **2000**, *328*, 363–368.
[29] P. M. Rafailov, J. Maultzsch, C. Thomsen, H. Kataura, *Phys. Rev. B* **2005**, *72*, 045411/1–7.
[30] M. Kalbac, L. Kavan, *J. Phys. Chem. C* **2009**, *113*, 16408–16413.
[31] M. Lazzeri, S. Piscanec, F. Mauri, A. C. Ferrari, J. Robertson, *Phys. Rev. B* **2006**, *73*, 155426/1–6.
[32] A. Das, A. K. Sood, A. Govindaraj, A. M. Saitta, M. Lazzeri, F. Mauri, C. N. R. Rao, *Phys. Rev. Lett.* **2007**, *99*, 136803/1–4.
[33] K. Yanagi, Y. Miyata, H. Kataura, *Adv. Mater.* **2006**, *18*, 437–442.
[34] L. Kavan, L. Dunsch, H. Kataura, A. Oshiyama, M. Otani, S. Okada, *J. Phys. Chem. B* **2003**, *107*, 7666–7675.
[35] T. Pichler, M. Matus, J. Kurti, H. Kuzmany, *Phys. Rev. B* **1992**, *45*, 13841–13844.
[36] M. Kalbac, H. Farhat, L. Kavan, J. Kong, M. S. Dresselhaus, *Nano Lett.* **2008**, *8*, 3532–3537.

Received: May 21, 2010
Published online: August 26, 2010

 © 2010 Wiley-VCH Verlag GmbH & Co. KGaA, Weinheim